

GPI-anchored receptor clusters transiently recruit Lyn and $G\alpha$ for temporary cluster immobilization and Lyn activation: single-molecule tracking study 1

Kenichi G.N. Suzuki,¹ Takahiro K. Fujiwara,¹ Fumiyuki Sanematsu,¹ Ryota Iino,¹ Michael Edidin,² and Akihiro Kusumi¹

¹Membrane Mechanisms Project, International Cooperative Research Project, Japan Science and Technology Agency (ICORP/JST), The Institute for Frontier Medical Sciences, Kyoto University, Kyoto, 606-8507, Japan

²Department of Biology, The Johns Hopkins University, Baltimore, MD 21218

The signaling mechanisms for glycosylphosphatidylinositol-anchored receptors (GPI-ARs) have been investigated by tracking single molecules in living cells. Upon the engagement or colloidal gold-induced cross-linking of CD59 (and other GPI-ARs) at physiological levels, CD59 clusters containing three to nine CD59 molecules were formed, and single molecules of $G\alpha i2$ or Lyn (GFP conjugates) exhibited the frequent but transient (133 and 200 ms, respectively) recruitment to CD59 clusters, via both protein–protein and lipid–lipid (raft) interactions.

Each CD59 cluster undergoes alternating periods of actin-dependent temporary immobilization (0.57-s lifetime; stimulation-induced temporary arrest of lateral diffusion [STALL], inducing IP_3 production) and slow diffusion (1.2 s). STALL of a CD59 cluster was induced right after the recruitment of $G\alpha i2$. Because both $G\alpha i2$ and Lyn are required for the STALL, and because Lyn is constitutively recruited to CD59 clusters, the STALL of CD59 clusters is likely induced by the $G\alpha i2$ binding to, and its subsequent activation of, Lyn within the same CD59 cluster.

Introduction

Stefanova et al. (1991) published one of the first papers showing that the cross-linking of a glycosylphosphatidylinositol-anchored receptor (GPI-AR), such as CD59 and decay accelerating factor (DAF), induces the formation of molecular complexes with Src-family kinases (SFKs) and their activation by phosphorylation (Shenoy-Scaria et al., 1992; Morgan et al., 1993). However, the GPI-ARs are located on the extracellular surface and are only anchored to the outer leaflet of the plasma membrane, and the SFKs are located in the cytoplasm or in/on the cytoplasmic leaflet of the cell membrane. Therefore, the mechanism by which GPI-ARs form complexes with SFKs and activate them has been a long-standing enigma. Because GPI-ARs and many SFKs tend to partition into the detergent-resistant membrane (DRM) fractions, the involvement of so-called raft microdomains in

GPI-AR-mediated signal transduction has been proposed (Simons and van Meer, 1988; Brown and Rose, 1992; Simons and Ikonen, 1997; Simons and Toomre, 2000; Brugger et al., 2004).

Furthermore, using immunofluorescence staining, Harder et al. (1998) found that when placental alkaline phosphatase (PLAP), a GPI-AR, was cross-linked, an SFK, Fyn (another putative raft-associating molecule, with myristoyl and palmitoyl anchoring chains), was recruited to the cross-linked PLAP in fibroblastic cells (the term recruit is used here for brevity, to indicate that the cytoplasmic molecules come and stay right beneath the cross-linked GPI-ARs). In addition, Gri et al. (2004) found that CD59 clustering in the outer leaflet induces the colocalization of CFP, anchored to the inner leaflet via two saturated chains in patches, in a cholesterol-dependent manner. Meanwhile, by using immunoprecipitation, Solomon et al. (1996) discovered the association of GPI-ARs (CD59, CD48, and Thy-1) with $G\alpha i2$ and $G\alpha i3$ in lymphocytes. Therefore, how $G\alpha$ is and SFKs on/in the cytoplasmic leaflet are recruited at cross-linked GPI-ARs in the outer leaflet, and how $G\alpha$ is and SFKs become activated, is one of the key issues in signal transduction studies of GPI-ARs.

These two lines of research converge because the activation of SFKs by the binding of $G\alpha$ s and $G\alpha$ i has been established. Ma et al. (2000) reported that $G\alpha$ s and $G\alpha$ i, but not $G\alpha$ q, $G\alpha$ 12,

Correspondence to Akihiro Kusumi: akusumi@frontier.kyoto-u.ac.jp

Abbreviations used in this paper: CCD, charge-coupled device; DAF, decay accelerating factor; DOPE, 1,2-dioleoyl-*sn*-glycero-3-phosphoethanolamine; DRM, detergent-resistant membrane; GPI-AR, glycosylphosphatidylinositol-anchored receptor; IP_3 , inositol-(1,4,5) triphosphate; LDL, low-density lipoprotein; MBCD, methyl- β -cyclodextrin; PLAP, placental alkaline phosphatase; PP2, 4-amino-5-[4-chlorophenyl]-7-(*t*-butyl)pyrazolo[3,4-*d*]pyrimidine; PTX, pertussis toxin; SFK, Src-family kinase; STALL, stimulation-induced temporary arrest of lateral diffusion; TCZ, transient confinement zone; TIRF, total internal reflection fluorescence.

The online version of this article contains supplemental material.

or $G\beta\gamma$, are the major activators for SFKs. With regard to SFK activation, there are several steps or different pathways. Dephosphorylation at the tyrosine residue near the C terminus (Y508 for Lyn) is usually necessary for the activation, and further activation is achieved by the phosphorylation of another tyrosine residue (Y397 for Lyn and Y418 for c-Src) in the activation loop, perhaps via autophosphorylation. However, Ma et al. (2000) showed another pathway *in vitro*: the binding of $G\alpha_s$ or $G\alpha_i$ to SFKs induces the activation of SFKs, without the need for dephosphorylation of the tyrosine near the C terminus. Therefore, we performed research based on a working hypothesis in which $G\alpha_i$ and SFKs are coincidentally recruited to GPI-AR clusters to form a complex, leading to SFK activation (Solomon et al., 1996; Ma et al., 2000). This working hypothesis is also consistent with the results of pull-down assays, showing the coupling of folate receptor $G\alpha_i3$ -Lyn or $G\alpha_i$ -Src (Minshall et al., 2000; Miotti et al., 2000). In this research, we mostly focused on CD59 as our model GPI-AR, but DAF and PLAP gave essentially the same results.

These pioneering studies collectively raise two further key questions. The first question is the recruitment dynamics of signaling molecules: how are $G\alpha_i$ and SFK molecules recruited to a CD59 cluster, and how long do they stay with the cluster for each recruitment event? We approached this problem by investigating the recruitment of cytoplasmic signaling molecules to GPI-AR clusters at the level of single molecules in living cells. By tracking single molecules in living cells, we should be able to learn how molecular interactions and recruitment take place in a spatiotemporally organized way. Conventional methods only observe the molecular events averaged over a large molecular ensemble, as well as over time and space, and therefore could easily miss dynamic and transient events.

The second question is whether previous observations might be a consequence of extensive aggregation of GPI-ARs induced by antibodies. Almost all of the receptor molecules on the cell surface might be cross-linked to form many large clusters. Therefore, we used colloidal gold particles with a 40-nm diameter, conjugated with whole IgG antibody, to induce clusters of a mean of six CD59 molecules. We also limited the number of gold particles attached to the cell to ~ 600 gold particles/cell, thus inducing the engagement of $\sim 4,000$ copies of CD59. Under these conditions, signaling responses comparable to those under physiological conditions were observed.

Others found that when raft-associating molecules were cross-linked with a colloidal gold particle with a 40-nm diameter, they exhibited alternating periods of apparently simple diffusion and temporary confinement within a zone (every 1–10 s; Sheets et al., 1997; Dietrich et al., 2002). These regions were termed transient confinement zones (TCZs). Based on these observations and our working hypothesis, we examined the possibility that TCZs might be induced by $G\alpha_i$ and/or SFKs recruited to gold-induced CD59 clusters.

We simultaneously tracked the movements of single GPI-AR clusters and single molecules of $G\alpha_i2$ and Lyn (an SFK). Our selections of $G\alpha_i2$, among the other $G\alpha$'s, and of Lyn, among the other SFKs, are based on the results by Solomon et al. (1996) and Ma et al. (2000), as well as on our immunofluorescence

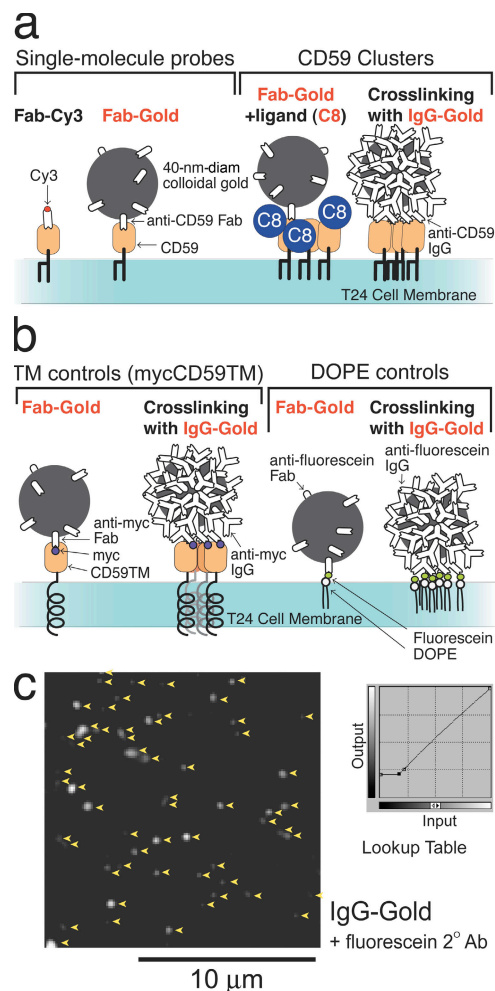


Figure 1. Probes used in this work. (a) Nonstimulated CD59 was observed using Cy3-conjugated anti-CD59 Fab (Fab-Cy3) and 40-nm-diameter gold particles conjugated with small numbers of anti-CD59 Fab fragments (Fab-gold), which hardly induced CD59 cross-linking. To observe CD59 engaged in signaling, CD59 was first tagged with a Fab-gold particle and then the ligand (C8) was added, or CD59 was cross-linked by 40-nm-diameter gold particles conjugated with anti-CD59 whole IgG (IgG-gold). (b) MycCD59TM, a transmembrane mutant of CD59, and fluorescein-labeled DOPE, an unsaturated phospholipid, were introduced in the plasma membrane, and the effects of cross-linking were examined. (c) The distribution of IgG-gold on the cell surface 5 min after IgG-gold addition (arrowheads). IgG-gold was stained with fluorescein-labeled secondary antibodies to enhance its image, to avoid nondetected IgG-gold and, hence, large variations in the signal intensity for each IgG-gold. Background subtraction was done as shown in the lookup table.

and biochemical results using the human epithelial T24 used in this study (see Results). We critically examined the timing of the recruitment of $G\alpha_i2$ and Lyn with respect to the occurrence of TCZs.

In this paper, we describe how the TCZ of CD59 clusters may be induced by dynamically and transiently recruiting individual $G\alpha_i$ and Lyn molecules at the cluster, and in the companion paper (see Suzuki et al. on p. 731 of this issue), we report the function of the TCZ. Experimental data, examining the involvement of raft microdomains in the signaling of GPI-ARs, are shown in many display items in this paper, but they are collectively discussed in Suzuki et al. (2007).

Results

Small numbers of CD59 clusters can elicit the bulk Lyn activation

In most of the experiments described here, the human epithelial cell line T24 was used. It expresses CD59, Gαi2, and Lyn, and therefore it is expected to undergo the nonlethal signaling responses found in immune cells upon the engagement of CD59 (Stefanova et al., 1991; Morgan et al., 1993). Because CD59 is ubiquitously expressed in most cells (Kimberley et al., 2007), the results obtained here would be useful in a wide variety of cells. Unless otherwise stated, all of the single-molecule tracking experiments were performed at 37°C. Various CD59 and control probes used in this work are shown in Fig. 1 (a and b).

Upon the addition of the cross-linking gold probe (IgG-gold; Fig. 1 a, right) at a concentration of 1.8×10^{10} particles/ml, 610 ± 54 (mean \pm SEM; $n = 9$ cells) particles/cell were bound to the T24 cell surface at 5 min after the probe addition, whereas almost all of the single-molecule and single-particle tracking experiments were performed within 5 min after the addition of the gold particle (Fig. 1 c). Almost all of them were found on the apical (dorsal) surface: the 40-nm gold particles probably did not readily enter the space between the bottom (ventral) membrane and the coverslip.

Such IgG-gold binding was sufficient to elicit intracellular signaling, at levels comparable to that induced by CD59's natural ligand, C8, at a serum (therefore high) concentration (at a cytolytic membrane attack complex unit of 1,000/coverslip; Jasin, 1977; Fig. 1 a, third from left). The amplitude and the time course of Lyn (and other SFKs) phosphorylation in its activation loop (at Y397, as detected by antibodies to phosphorylated Y418 of c-Src) after the binding of ~ 600 IgG-gold probes were similar to those after C8 addition (Fig. 2, a and b; Murray and Robbins, 1998). The intracellular inositol-(1,4,5) triphosphate (IP₃)-Ca²⁺ responses upon the additions of IgG-gold or C8 were also very similar to each other (see Figs. 1–3 in Suzuki et al., 2007).

These results show that CD59 could act as a signaling receptor in epithelial cells, like in immune cells, as well as a complement control factor (Stefanova et al., 1991; Morgan et al., 1993). The IgG-gold-induced signaling was specific with regard to GPI-anchoring and cross-linking. Multivalent gold probe-induced cross-linking of a transmembrane mutant of CD59 (mycCD59TM; CD59 with a myc tag at its N terminus and the transmembrane domain plus the following 12 amino acids of the low-density lipoprotein (LDL) receptor attached at its C terminus; De Nardo et al., 2002; Fig. 1 b, left; 560 ± 51 particles attached per cell; $n = 5$ cells) and a nonraft phospholipid, 1,2-dioleoyl-*sn*-glycero-3-phosphoethanolamine (DOPE; Fig. 1 b, right; 670 ± 48 particles attached per cell; $n = 8$ cells), did not induce intracellular signaling responses. Control gold particles (Fab-gold; Fig. 1 a, left), prepared by conjugating small numbers of Fab fragments of the anti-CD59 antibody to gold particles, did not elicit either Lyn activation (Fig. 2 b) or IP₃-Ca²⁺ signaling (see Figs. 1–3 in Suzuki et al., 2007). (This in itself strongly supports the proposal that Fab-gold is not cross-linking.)

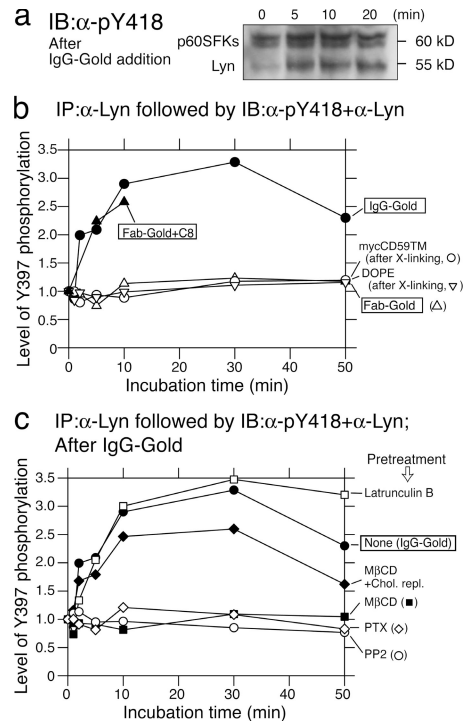


Figure 2. Clustering of CD59 by IgG-gold or C8 induced phosphorylation of SFKs, including Lyn, in their activation loops. (a) The level of SFK phosphorylation after IgG-gold addition, as shown in a Western blot with anti-pY418-Src antibodies (recognizing Lyn phosphorylation at Y397). The bottom bands are Lyn, and the top bands are p60SFKs (c-Src, Yes, and Fyn), as identified by reprobing with each respective antibody. (b) The ratio of activated Lyn to total Lyn (immunoblotting with anti-pY418 versus that with anti-Lyn; arbitrary units) plotted against the incubation time. (c) Time courses of Lyn phosphorylation after IgG-gold addition after various pretreatments of cells at 37°C: 50 nM latrunculin B, 4 mM MβCD (and also the subsequent cholesterol replenishment with 10 mM MβCD-cholesterol), 10 μM PP2 (SFK blocker), and 1.7 nM PTX (Gα blocker; 10 min, 30 min, 5 min, and 22 h, respectively). All of the SEMs for the points plotted here are within 30% of the given value. The overall amounts of cholesterol per cell after cholesterol depletion and after the subsequent replenishment were found to be 66 and 118% of the original amount (SD of $\pm 6\%$).

An independent observation further indicated that Fab-gold practically does not cross-link CD59, although one should be aware that 20–40% of GPI-anchored proteins may be in clusters smaller than pentamers, with the remaining 60–80% being monomers (Sharma et al., 2004). The diffusion coefficient of Fab-gold attached to CD59, observed by single-particle tracking on a 100-ms time scale ($D_{100\text{ms}}$, corresponding to $D_{2.4}$ in Kusumi et al., 1993), was the same as that for Fab-Cy3-labeled CD59, estimated by single fluorescent molecule tracking (Fig. 1 a, left; 0.19 vs. 0.20 $\mu\text{m}^2/\text{s}$, respectively), whereas the single fluorescent molecule tracking method is sensitive to the difference between IgG-Cy3-labeled CD59 and Fab-Cy3-labeled CD59 (median of 0.09 and 0.20 $\mu\text{m}^2/\text{s}$, respectively; $P < 0.01$).

The $D_{100\text{ms}}$ of IgG-gold is only half that of Fab-gold after C8 addition (in median values of 0.022 vs. 0.042 $\mu\text{m}^2/\text{s}$, respectively; the Fab-gold $D_{100\text{ms}}$ decreases from 0.19 to 0.042 $\mu\text{m}^2/\text{s}$ upon C8 addition), suggesting that the sizes of the IgG-gold-induced CD59 clusters are only slightly greater than those of Fab-gold + C8, based on the concept of oligomerization-induced trapping within the membrane skeleton mesh, as proposed by

Iino et al. (2001) (Fig. S1, available at <http://www.jcb.org/cgi/content/full/jcb.200609174/DC1>). Therefore, the CD59 cluster size beneath the cross-linking IgG-gold may be comparable to that induced by C8 addition (Fig. 1 a, right).

Three to nine CD59 molecules may be clustered beneath a single IgG-gold particle

Single fluorescent molecule tracking revealed that a fluorescent spot representing the complex of five Cy3 anti-CD59-IgG antibody molecules and CD59 (clustered by a secondary antibody and not the IgG-gold), namely, a spot containing 5–10 molecules of CD59, was practically immobile (Fig. S2, available at <http://www.jcb.org/cgi/content/full/jcb.200609174/DC1>). As our IgG-gold probes attached to the cell surface were still mobile, this indicates that the number of CD59 molecules beneath an IgG-gold particle would be <10. Meanwhile, the diffusion coefficient $D_{100\text{ms}}$ of IgG-gold (median = $0.022 \mu\text{m}^2/\text{s}$) is smaller than those for Fab-gold ($0.19 \mu\text{m}^2/\text{s}$) and IgG-Cy3-labeled CD59 (median = $0.09 \mu\text{m}^2/\text{s}$) by factors of approximately nine and four, respectively, suggesting that IgG-gold may cross-link more than two CD59 molecules. Therefore, it would be safe to conclude that an IgG-gold-induced CD59 cluster contains three to nine molecules of CD59, with six CD59 molecules/IgG-gold-induced cluster as a reasonable number to use, although these IgG-gold-induced clusters may contain other recruited proteins. The terms CD59 cluster and GPI-AR cluster are used with this understanding. It follows that ~ 600 hexameric (mean) CD59 clusters, totaling $\sim 3,600$ CD59 molecules per cell, on average, are clustered or engaged in the present work, and that this will be sufficient to trigger robust intracellular SFK activation and calcium mobilization at physiological levels.

CD59 clusters often undergo temporary immobilization

We next observed the movement of each individual Fab-gold (before and after the C8 addition; Fab-gold-C8) and IgG-gold on the cell surface at video rate (33 ms/frame; Fig. 3 a and Video 1, available at <http://www.jcb.org/cgi/content/full/jcb.200609174/DC1>). Both Fab-gold-C8 and IgG-gold exhibited apparently simple, but slow, diffusion (at a 300-fold-enhanced frame rate of 0.11 ms/frame, both probes exhibited hop diffusion, with a mean compartment size comparable to that found previously by Murase et al. [2004]; median = 110 nm, at a mean hop rate of once every 200 ms [$n = 37$]). However, in addition to this apparent simple diffusion observed at video rate, both Fab-gold-C8 and IgG-gold were often temporarily immobilized, as seen in the trajectories in Fig. 3 a, as statistically detected by software designed to find TCZs (Simson et al., 1995; Sheets et al., 1997; Dietrich et al., 2002; Chen et al. 2006; Fig. S3, available at <http://www.jcb.org/cgi/content/full/jcb.200609174/DC1>; and Table I). As shown in Table I and in Suzuki et al. (2007), our results indicate that these temporary immobilization events might be induced by the binding of CD59 clusters to actin filaments (must be bound indirectly) and/or actin-associated membrane microdomains, because they are inhibited by partial depolymerization of actin filament (Table I); therefore, to avoid ruling out the

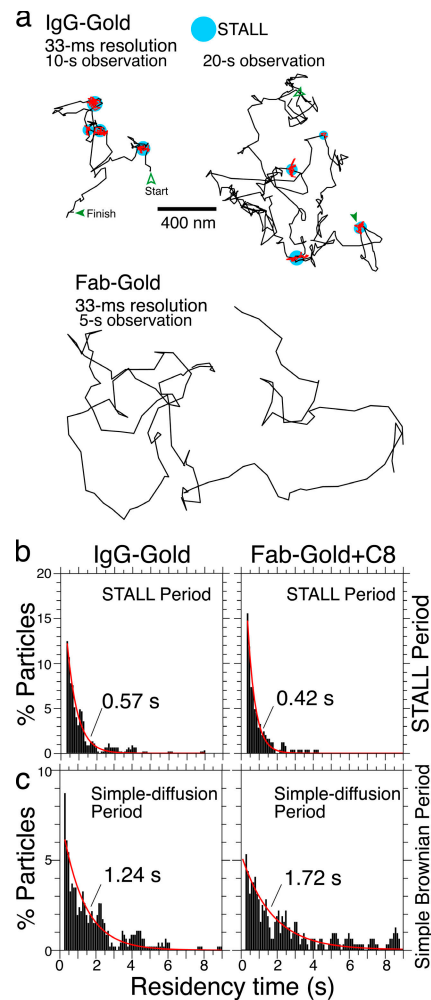


Figure 3. CD59 clusters undergo alternating periods of STALL and apparently simple diffusion. (a, top) Typical trajectories of IgG-gold recorded at video rate. CD59 clusters exhibit alternating periods of apparently simple Brownian diffusion (black trajectories) and STALL (magenta trajectories in the circular blue areas). See Video 1 (available at <http://www.jcb.org/cgi/content/full/jcb.200609174/DC1>) for the trajectory on the right. (bottom) A representative trajectory of Fab-gold recorded at video rate, shown for comparison with those of IgG-gold. (b and c) Histograms showing the distributions of the STALL and diffusing periods, respectively, of IgG-gold (left) and Fab-gold + C8 (right; magenta curves indicate the best exponential fits).

possibility of actin binding (rather than partitioning into zones), we call this temporary immobilization stimulation-induced temporary arrest of lateral diffusion (STALL). Both Fab-gold-C8 and IgG-gold intermittently exhibited STALL, separated by periods of apparently simple Brownian diffusion. The distributions of the durations of STALL and simple diffusion are shown in the histograms shown in Fig. 3 (b and c), which could be fitted with single exponential decay curves, giving the characteristic lifetimes (exponential decay constants) for the STALL and mobile periods of 0.57 and 1.2 s, respectively, for IgG-gold. This would predict that IgG-gold is in the STALL period $\sim 32\%$ of the time. Actually, as shown in Table I, IgG-gold exhibited STALL for 162 s out of the total observation period of 440 s, or 36% of the total observation time. The CD59 clusters induced by the binding of C8 (Fab-gold-C8) exhibited STALL for 17% of the

Table I. Lyn phosphorylation in the activation loop, and the temporal fraction, frequency, and exponential lifetime of CD59's STALL, evaluated under various conditions

Probes and pretreatments	Relative Lyn activation ^a (10 min after ligand addition)	Temporal fraction in STALL ^b	Frequency of STALL ^b	Exponential lifetime of STALL ^c	<i>n</i>
		%	min ⁻¹	s	
Fab-gold	1	4.5	6.5	0.20	107
Fab-gold + C8	2.6	17	12	0.42	41
IgG-gold (~610 particles bound/cell)	2.9	36	19	0.57	44
IgG-gold					
+ Cholesterol depletion with MβCD	0.8	7.6	6.9	0.36	49
+ Subsequent cholesterol repletion	2.5	28	18	0.50	26
+ Cholesterol depletion with 60 μg/ml saponin	ND	14	11	0.39	52
+ Actin depolymerization ^d	3.0	4.2	7.1	0.21	32
+ Inhibition of SFK	1.0	8.2	8.4	0.29	88
+ Inhibition of Gαi2	1.2	12	10	0.40	71
mycCD59TM, crosslinked by IgG-gold (~560 particles bound/cell)	0.9	4.9	3.5	0.27	55
DOPE monomers	ND	3.1	4.8	0.20	89
DOPE, crosslinked by IgG-gold ^e (~670 particles bound/cell)	1.0	4.0	5.5	0.17	23

Numbers in bold indicate that the STALL mechanism may be different in these cases. See Fig. 2.

^aThe maximal error in this measurement was ±30% of the given value.

^bThe results of direct observations rather than the calculated value from the lifetimes for STALL and apparently simple Brownian diffusion.

^cThe maximal SEM in this measurement was ± 0.04 s.

^dPartial actin depolymerization was carried out by incubating the cells in the medium containing 50 nM latrunculin B for 10 min.

^eDOPE concentrations (0.3–30 μg/ml of DOPE was preincubated with the cells) and the number of IgG molecules on a gold particle (1- to 20-fold of the minimal protecting amount) were systematically varied, and the maximal STALL fraction is listed here.

observation time (67 s out of 410 s), whereas nonstimulated CD59 molecules (Fab-gold) were temporarily immobilized for only 4.5% of the observation time (24 s out of 535 s). In contrast, DOPE or mycCD59TM, non-DRM/non-putative raft molecules, did not exhibit STALL behavior, even after cross-linking by IgG-gold particles (Table I). For further discussion of membrane compartments and STALL, with their detection with a higher time resolution of 0.11 ms, see Fig. S4. None of the STALL sites were colocalized with caveolae, as marked by caveolin 1–GFP, under the experimental conditions used here (only the initial events, generally within 5 min after IgG-gold addition were observed). For further data, see Fig. S5.

Involvement of Lyn in STALL induction of CD59 clusters

The following four observations suggested the involvement of Lyn in inducing STALL of CD59 clusters, formed by IgG-gold particles. First, after the cells were treated with the SFK inhibitor 4-amino-5-(4-chlorophenyl)-7-(*t*-butyl)pyrazolo[3,4-*d*]pyrimidine (PP2) or pertussis toxin (PTX), an inhibitor for Gαi's, both the Lyn activation (Lyn phosphorylation at Tyr397) and STALL occurrence were inhibited (Fig. 2 c and Table I). These results suggest that the activities of Lyn and Gαi's are required for inducing STALL (according to Ma et al. [2000], Lyn is activated by the direct binding of Gαs and Gαi). Second, other GPI-ARs (PLAP and DAF) in T24 cells or CD59 in other cell lines (NRK and PtK2) also exhibited PP2-dependent STALL, indicating the SFK requirement for inducing STALL (Table II). Third, the temporal fraction of the CD59 cluster in STALL was only 2.8% in SYF cells, which do not express Lyn,

Src, Yes, Fyn, and other SFKs, but the STALL temporal fraction increased to 20% after Lyn expression (Table III). In addition, IgG-gold on YF cells, which do express c-Src but not other SFKs, exhibited a 9.6% temporal fraction of STALL. DOPE, a nonraft molecule, did not exhibit a significant level of STALL under any conditions (Table III). These results indicate the necessity of Lyn activity (or c-Src and other SFK activity) for the induction of STALL. Fourth, the treatment of cells with methyl-β-cyclodextrin (MβCD) or saponin, for partial depletion or clustering of cholesterol, blocked both the Lyn activation and STALL of the CD59 clusters. Furthermore, the subsequent replenishment of cholesterol with cholesterol-loaded MβCD reinstated both the Lyn activation and STALL of the CD59 clusters (Fig. 2 c and Table I), showing the high correlation between the STALL occurrence and Lyn activation (see Discussion in Suzuki et al., 2007).

These observations led us to propose a model in which Lyn is recruited to the molecular complex centered on CD59 clusters and is activated in the molecular complex (by the binding of Gαi2 as described later) and, in turn, induces STALL by phosphorylating as-yet-unknown proteins, which might mediate the binding of CD59 clusters to actin filaments or to domains supported by actin filaments (Table I and Fig. 4 in Suzuki et al., 2007).

Single-molecule tracking shows that Lyn is dynamically/transiently recruited to CD59 clusters

We simultaneously observed each individual CD59 cluster and single molecules of Lyn-GFP (known to be functional; Kovarova

Table II. The temporal fraction, frequency, and lifetime of STALL for different GPI-ARs in different cell lines (in addition to CD59 in T24 cells) under various conditions

Cell type, GPI-AR, and various pretreatments	Temporal fraction in STALL ^a	Frequency of STALL ^a	Exponential lifetime of STALL ^b	<i>n</i>
	%	min ⁻¹	s	
NRK cell-CD59 ^c				
Fab-gold	1.8	1.3	ND ^d	27
IgG-gold	19	15	0.42	58
IgG-gold with pretreatments				
+ Cholesterol depletion	1.9	1.2	0.20	50
+ Actin depolymerization	1.6	1.8	0.27	52
+ Inhibition of SFK	5.0	5.8	0.25	49
PtK2 cell-CD59 ^c				
Fab-gold	4.0	2.7	ND ^d	20
IgG-gold	23	17	0.51	34
IgG-gold with pretreatments				
+ Cholesterol depletion	4.2	4.6	0.28	35
+ Actin depolymerization	9.4	9.7	0.24	55
+ Inhibition of SFK	8.1	11	0.24	30
T24 cell-PLAP				
Fab-gold	3.3	2.0	ND ^d	35
IgG-gold	15	12	0.44	34
IgG-gold with pretreatments				
+ Cholesterol depletion	5.0	5.7	0.26	45
+ Actin depolymerization	2.9	3.4	0.19	35
+ Inhibition of SFK	5.2	6.5	0.24	52
T24 cell-DAF				
Fab-gold	1.1	1.7	ND ^d	59
IgG-gold	23	15	0.55	71
IgG-gold with pretreatments				
+ Cholesterol depletion	4.6	5.4	0.26	70
+ Actin depolymerization	4.0	5.0	0.22	63
+ Inhibition of SFK	3.8	4.9	0.21	60

^aThe results of direct observations rather than the calculated value from the lifetimes for STALL and apparently simple Brownian diffusion.

^bThe maximal SEM in this measurement was ± 0.04 s.

^cAlthough these cells express CD59, to use the same mouse monoclonal antibody to human CD59, human CD59 was expressed in NRK and PtK2 cells, and the amounts of added IgG-gold particles were adjusted so that about the same number of particles as in T24 cells was found in these cell types.

^dNot analyzed because the STALL number was very small.

et al., 2001) expressed in T24 cells (Fig. 4 a). For such observations, 50-nm latex particles, rather than 40-nm colloidal gold particles, were used to form CD59 clusters, to avoid the signal from the gold particles (see Materials and methods). Fig. 4 b shows typical trajectories of a CD59 cluster (black), including four STALL periods, and a single Lyn-GFP molecule (orange trajectory), including a period of colocalization (the magenta part of the Lyn-GFP trajectory and the indigo part of the CD59 cluster trajectory; Video 2, available at <http://www.jcb.org/cgi/content/full/jcb.200609174/DC1>). Lyn-GFP is generally located on the cytoplasmic surface of the membrane and is recruited at diffusing CD59 clusters by lateral diffusion on the cytoplasmic surface. However, this Lyn recruitment occurred with no correlation with the STALL of CD59 clusters (Fig. 4 b).

Based on many such experiments, we obtained a histogram of the time difference between the onset of STALL of a CD59 cluster (time 0) and the recruitment of a single Lyn-GFP molecule to that particular CD59 cluster (Fig. 5, a and b). The number of incidental overlaps of a Lyn-GFP spot with a CD59 cluster, estimated by up-shifting the CD59 cluster video sequence

by 50 video frames (1.67 s), was subtracted (see Materials and methods). This histogram clearly indicates that Lyn is frequently recruited to CD59 clusters but without any correlation with the STALL events. This lack of a temporal correlation between the Lyn-GFP recruitment to a CD59 cluster and the induction of the CD59's STALL was surprising because Lyn is required for STALL induction, as described in the previous subsection (Tables I–III).

Single fluorescent molecule tracking shows that STALL of CD59 clusters takes place right after the transient recruitment of G α i2

The Lyn recruitment results (Fig. 5 b) suggest that, although Lyn activity is needed for inducing STALL (Tables I–III), an upstream molecule that activates Lyn may also have to be recruited to the same CD59 cluster for inducing its STALL. Lyn can be activated by the binding of G α s and G α i, but not G α q, G α 12, or G β γ , without dephosphorylating the tyrosine residue Y508 near the C terminus (Ma et al., 2000). In fact, we made three observations that suggest the involvement of G α i2 in Lyn

Table III. Lyn or c-Src can induce STALL of CD59 clusters

Cell lines and cross-linked molecules	Temporal fraction in STALL	Frequency of exhibiting STALL	<i>n</i>
	%	<i>min</i> ⁻¹	
SYF cells ^a			
CD59	2.8	1.2	43
DOPE	4.1	5.5	34
YF cells ^b			
CD59	9.6	9.5	31
DOPE	5.2	6.7	45
SYF cells transfected with Lyn			
CD59	20.2	12.7	36
DOPE	2.8	3.7	31

Although both SYF and YF cells express CD59, to use the same mouse monoclonal antibody for human CD59, human CD59 was expressed in these cells, and the amounts of added IgG-gold particles were adjusted so that about the same number of particles as in T24 cells were found in these cell types. For the DOPE experiments, see Table I.

^aSYF cells do not express c-Src, Fyn, Yes, or Lyn.

^bYF cells express c-Src, but not Fyn, Yes, or Lyn.

activation and the STALL of CD59 clusters. (1) In the biochemical experiment shown in Fig. 2 c, we found that IgG-gold-induced Lyn activation is blocked by PTX, a Gαi blocker. (2) PTX also blocked the STALL of CD59 clusters (Table I). (3) Immunofluorescence observations revealed a certain level of colocalization of Gαi2 with CD59 clusters (Figs. 6 and 7; but much less in the case of Gαi1, Gαi3, and Gαs, perhaps because of their low expression levels; not depicted). Because PTX totally blocked the IgG-gold-induced Lyn activation, it is difficult to conceive any pathways of Lyn activation other than those

mediated by Gαi's. Based on these observations, we formed a working hypothesis in which Gαi2 is also recruited to CD59 clusters, and when it encounters Lyn at the CD59 cluster, it binds and activates Lyn there, inducing STALL of the CD59 cluster by its binding to an actin filament. Therefore, we examined Gαi2 recruitment to CD59 clusters.

We simultaneously observed single molecules of Gαi2(YFP) and CD59 clusters (Fig. 4 c). A typical trajectory of a CD59 cluster that includes a STALL period (Fig. 4 d, blue), as well as a period of colocalization with a single Gαi2(YFP) molecule (the magenta part of the Gαi2[YFP] trajectory and the indigo part of the CD59 cluster trajectory), is shown in Fig. 4 d (Video 3, available at <http://www.jcb.org/cgi/content/full/jcb.200609174/DC1>). First, note that, at variance with the general concept of higher membrane localization of trimeric G proteins and Gαi2 than in the cytoplasm, and also in contrast to Lyn-GFP, the residency time of Gαi2(YFP) on the cytoplasmic surface of the plasma membrane is short, on the order of 100 ms (Video 4), consistent with the observations made by Yu and Rasenick (2002) and Frank et al. (2005). The colocalized Gαi2(YFP) molecules usually stayed on the membrane only during the colocalization period or longer by only a few video frames. Gαi2(YFP) molecules must be frequently colliding with the inner surface of the plasma membrane, but they were invisible at video rate because they rarely stay on the membrane longer than a video frame time of 33 ms. They stay longer (median of 133 ms) when they bump into CD59 clusters.

Interestingly, the recruitment of a Gαi2(YFP) molecule to the CD59 cluster took place right before the beginning of STALL, as exemplified by the trajectories shown in Fig. 4 d. The distribution of the time difference between the recruitment of

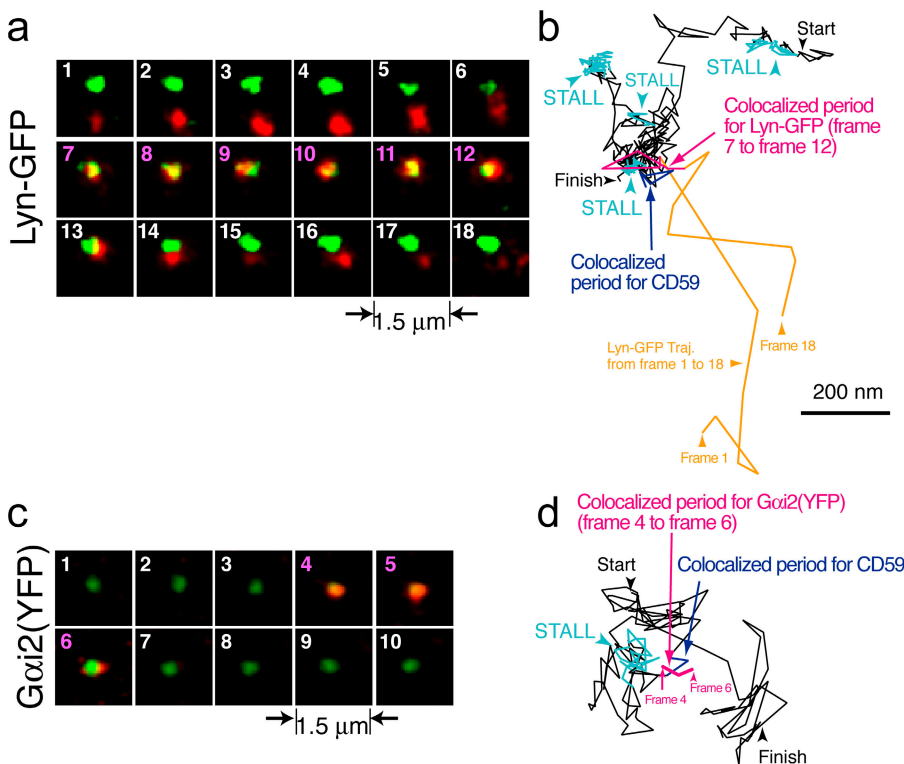


Figure 4. **Single-molecule detection of the transient recruitment of Lyn-GFP and Gαi2(YFP) to CD59 clusters.** (a and c) Image sequences showing superimposed video frames of simultaneous recordings of a CD59 cluster (induced by a 50-nm latex particle, which was observed by a bright-field microscopy; green) and single molecules of Lyn-GFP (a) or Gαi2(YFP) (c; red). Gaussian spatial smoothing was applied to the images. A single Lyn-GFP [Gαi2(YFP)] molecule was colocalized from frame 7 until 12 in panel a (frame 4 until 6 in c; indicated by pink frame numbers). (b and d) A typical trajectory of a CD59 cluster (black), including STALL periods (the blue parts of the trajectories) and a period in which it was colocalized with Lyn-GFP or Gαi2(YFP) (magenta part in the otherwise orange trajectory; it overlaps with a STALL site but at different times). See Videos 2 and 3 (available at <http://www.jcb.org/cgi/content/full/jcb.200609174/DC1>) for the original video sequences for Lyn-GFP (a and b) and Gαi2(YFP) (c and d) shown here, respectively. Colocalization was defined by Koyama-Honda et al. (2005).

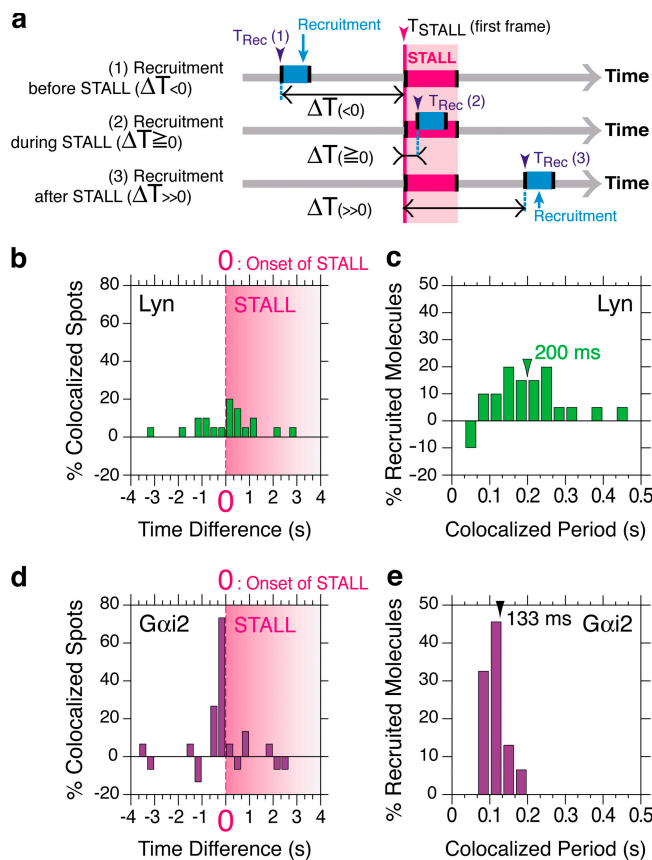


Figure 5. Lyn-GFP is dynamically recruited at CD59 clusters, without any time correlation with STALL, whereas Gai2(YFP) colocalization, which is also transient, occurs right before the onset of STALL. (a) The definition of the time difference (lag time = ΔT) between the recruitment of a single molecule of Lyn-GFP (or Gai2[YFP]) and the onset of STALL (time = 0). It was defined as the first frame of Lyn-GFP (or Gai2[YFP]) recruitment to a CD59 cluster (T_{Rec}) minus the first frame of the nearest STALL (T_{STALL}). (b and d) The distribution of the time difference (ΔT) between the recruitment of a single molecule of Lyn-GFP (b) (or Gai2[YFP]; panel d) and the onset of STALL. Each STALL period starts at time 0 but ends at different times (the pink shade showing STALL is, thus, graded). The frequency of incidental colocalization events was evaluated by artificially shifting the CD59 cluster video sequence by 50 frames (1.67 s) and was subtracted (see Materials and Methods). (c and e) The distribution of the colocalization duration of single molecules of Lyn-GFP (c) or Gai2(YFP) (e) at CD59 clusters (medians are shown).

Gai2(YFP) to a CD59 cluster and the onset of STALL (Fig. 5 d) clearly indicates that right after the recruitment of a Gai2(YFP) molecule to a CD59 cluster, its STALL is initiated, showing a marked contrast with the Lyn recruitment. These results, therefore, are consistent with our working hypothesis, in which the CD59 cluster provides a platform for temporarily recruiting Lyn and Gai2 and for inducing Lyn activation by the binding of newly recruited Gai2. Such dynamics would never have been revealed by normal imaging or biochemical methods.

The residency times for each recruited Gai2 and Lyn molecule at a CD59 cluster are 100–200 ms

The colocalization period of Lyn-GFP at a CD59 cluster was 200 ms (median length of 6 video frames; Fig. 5 c). Because this recruitment duration is substantially shorter than the GFP

lifetime before photobleaching and blinking in the plasma membrane (~ 850 ms), these are not responsible for the short residency time. Therefore, Lyn-GFP molecules are joining and leaving the CD59 clusters continually and rapidly. Very similar observations were made with the recruitment of Gai2(YFP) to CD59 clusters. The duration of Gai2(YFP) colocalization with a CD59 cluster is even shorter, ~ 133 ms (median of 4 video frames; Fig. 5 e). Short-term recruitment of cytoplasmic molecules to the plasma membrane was also reported previously (Mashanov et al., 2004).

These results indicate that the recruitment of Gai2 and Lyn molecules at a CD59 cluster takes place quite dynamically. However, as described in previous subsections, the physiological CD59 clusters formed by C8 addition are even slightly smaller than those induced by IgG-gold. Therefore, such dynamic recruitment and short dwelling times are not likely to be artifacts as a result of the small sizes of CD59 clusters. Because Lyn activation lasts for >30 min, we initially assumed that each Lyn molecule stays at a CD59 cluster for at least several minutes and were surprised to find the recruitment period of ~ 200 ms on average. However, from the viewpoint of regulating the periods and levels of overall Lyn activation, simple addition of many such short recruitment events would be easier than carrying out complex integration of prolonged activation of individual molecules (see Fig. 8 in Suzuki et al., 2007).

Lyn recruitment depends on both lipid anchoring and protein–protein interactions

The frequency of transient single-molecule recruitment of Lyn-GFP to CD59 monomers, clusters, and mycCD59TM clusters (per minute), normalized by the number density of Lyn-GFP on the plasma membrane (justified because Lyn-GFP recruitment to CD59 always occurs in the membrane), is summarized in Table IV. The Lyn-GFP recruitment frequency to the CD59 cluster is about eightfold greater than that of non-cross-linked CD59 or the mycCD59TM cluster. This result is somewhat consistent with the results shown in Table I, in which the temporal fraction in STALL and the frequency of STALL were increased by factors of approximately eight and three, respectively, as CD59 was clustered.

To examine the relative importance of lipid–lipid and protein–protein interactions in the recruitment of Lyn-GFP to CD59 clusters (Douglass and Vale, 2005), the recruitment of LynN20-GFP, the N-terminal 20-amino-acid sequence of Lyn, which contains the binding sites for a palmitoyl and a myristoyl chain, fused at its C terminus to GFP (Pyenta et al., 2001), was examined. LynN20-GFP is recruited to the CD59 cluster 2.4 times less often than Lyn-GFP but 3.3 times more often than the controls (Lyn-GFP to non-cross-linked CD59 or to the mycCD59TM cluster). Furthermore, the residency durations of LynN20-GFP at CD59 clusters and Lyn-GFP at mycCD59TM clusters are considerably shorter than that of Lyn-GFP at CD59 clusters (unpublished data). These results suggest that both lipid–lipid interactions via Lyn’s alkyl chains and protein–protein interactions by way of Lyn’s protein moiety contributed to the recruitment of Lyn to the CD59 cluster. Furthermore, single molecules of transferrin receptor, a typical nonraft transmembrane

Table IV. Frequency of Lyn-GFP and LynN20-GFP recruitment to CD59 clusters, normalized by the number density of Lyn-GFP (or LynN20-GFP) spots on the plasma membrane

Lyn and its analogue	CD59 and its analogues	Number of recruitment events/min/number density of Lyn-GFP (or LynN20-GFP) spots on the membrane ^a	Overall length of the examined trajectories of CD59 (or its analogues)
Lyn-GFP	Non-cross-linked CD59	1.8	<i>min</i> 28.6
	mycCD59 TM cluster	1.9	17.5
	CD59 cluster	15.2	7.0
LynN20-GFP	CD59 cluster	6.4	8.0

^aThe number of incidental overlaps was subtracted, as described in the text and Materials and Methods in Suzuki et al. (2007). The normalization by the number density of Lyn-GFP (or LynN20-GFP) spots on the membrane can be justified because Lyn-GFP and LynN20-GFP almost always became colocalized with CD59 clusters from within the plasma membrane (rather than from the cytoplasm; these molecules may partition into both the cytoplasm and inner leaflet of the plasma membrane. The number of Lyn-GFP molecules observed on the plasma membrane at video rate recordings was not affected by cross-linking CD59).

protein, labeled with Alexa488-conjugated transferrin, were not significantly recruited to CD59 clusters, suggesting the involvement of “raft-dependent” mechanism for Lyn recruitment and excluding the possibilities of membrane accumulation beneath the CD59 clusters (Glebov and Nichols, 2004).

Colocalization of Lyn and Gαi2 to each other at CD59 clusters, observed by conventional immunofluorescence microscopy

First, we extensively cross-linked CD59 by the successive addition of anti-CD59 IgG and secondary antibodies and found that CD59 aggregates were colocalized by Lyn (Fig. 6, left), Gαi2 (middle), or both (right). Note the extensive CD59 aggregation, which is the condition often used for triggering the intracellular signaling. Second, using IgG-gold particles, we observed that ~20 and 10% of IgG-gold particles were colocalized with Lyn (as well as pY418) and Gαi2, respectively (Fig. 7, a and b). Noting that the immunofluorescence result represents a spatio-temporal mean of dynamic events occurring over the periods needed for chemical fixation and over a diffraction-limited space of ~400 nm, such low levels of colocalization are consistent with the transient recruitment of Lyn and Gαi2 at CD59 clusters. Namely, the dynamic, transient recruitment of Lyn and Gαi2 should not be considered inconsistent with their extensive immunocolocalization to each other at the large CD59 clusters (Fig. 6), Fyn colocalization with PLAP clusters (Harder et al., 1998), or colocalization of Lyn and Gαi2 at IgG-gold particles (Fig. 7, a and b).

Both PTX, a Gαi blocker, and PP2, an SFK blocker, reduced Lyn recruitment by about twofold (Fig. 7 b, middle), whereas they further blocked enhanced Lyn activation at CD59 clusters by four- to fivefold (pY418; Fig. 7 b, top). These results suggest that, upon the activation of Lyn at the CD59 clusters, the activated Lyn stays at the CD59 clusters longer than non-activated Lyn molecules by a factor of approximately two. Blocking of SFK activation by PP2 did not affect the Gαi2 recruitment. Fluorescein-DOPE, a typical nonraft phospholipid, preincorporated into the plasma membranes before the addition of IgG-gold, was not concentrated in the CD59 cluster domains (Fig. 7 a), indicating that membrane concentration and membrane undulations, as reported by Glebov and Nichols (2004), are not involved in the colocalization of Lyn and Gαi2 found here.

The low levels of immunocolocalization of Lyn and Gαi2 with IgG-gold-induced CD59 clusters, 20 and 10%, respectively, suggest that the colocalization of Lyn and Gαi2 to each other at the same IgG-gold-induced CD59 cluster (three-way colocalization) occurs rarely in the immunocolocalization observations. The three-way quantitative immunocolocalization results (non-single-molecule experiments) showed that ~4% of the CD59 clusters were colocalized with both Lyn and Gαi2, which is to be compared with the result after MβCD treatment, exhibiting ~1% three-way colocalization (Fig. 7, c and d). The comparison of these results with those using antibody-induced large-scale CD59 clusters (extensive colocalization of Lyn and Gαi2) suggests that an increase in the cluster size would enhance the total number of recruited Lyn molecules during a unit time but possibly without prolonging the residency time of each recruited Lyn molecule.

Discussion

We found that robust SFK phosphorylation (Fig. 2, b and c), increases in IP₃ concentration, and Ca²⁺ mobilization (Suzuki et al., 2007) were induced after the binding of ~600 IgG-gold particles to the cell surface, which probably engage ~3,600 CD59 molecules. Gold probe-induced cross-linking of mycCD59TM or DOPE (again, ~600 gold particles were bound to the cells), which are putative nonraftophilic molecules, did not trigger any observable intracellular signals (Fig. 2 b).

CD59 clusters undergo alternating periods of apparent simple Brownian diffusion (1.2-s lifetime) and STALL (0.57-s lifetime). As described (Suzuki et al., 2007), STALL is likely to be a key, but temporary, site for relaying the extracellular CD59 signal to the intracellular Ca²⁺ signaling pathways. Namely, single-molecule tracking found that PLCγ2 molecules are recruited to CD59 clusters only during the STALL periods, and various blocking experiments suggested that PLCγ2 molecules recruited to the STALLED CD59 clusters might produce IP₃ from PIP₂, which leads to the release of Ca²⁺ through the IP₃ channel located in the ER membrane. In the present paper, we describe how STALL is induced after the engagement of CD59.

Both Gαi2 and Lyn are necessary for inducing STALL of CD59 clusters (Table I). In the cell line lacking SFKs, STALL could not be induced, but STALL was reinstated after transfecting Lyn (Table III). Because PP2, an SFK blocker, inhibited STALL,

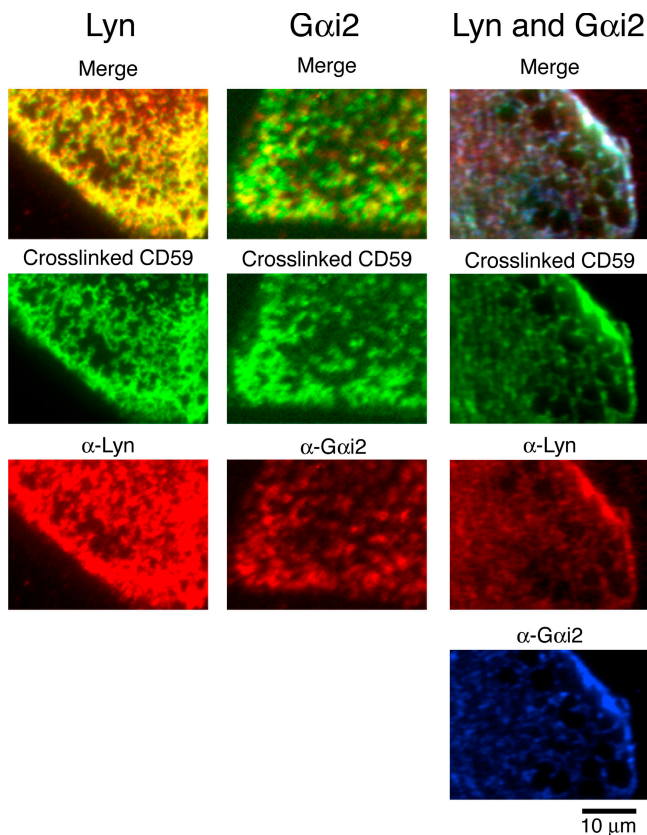


Figure 6. **Immunofluorescence colocalization of Lyn and Gai2 with CD59 cross-linked by primary and secondary antibodies.** After CD59 was extensively cross-linked by antibodies, cells were fixed with 4% paraformaldehyde and stained with anti-Lyn and/or anti-Gai2 antibodies.

Lyn phosphorylation in its activation loop may be mediated by autophosphorylation after the initial Lyn activation by Gai2 (Kmieciak and Shalloway, 1987).

Single-molecule tracking revealed the recruitment of Gai2 and Lyn molecules to CD59 clusters. Surprisingly, this occurs transiently (median of 133 and 200 ms, respectively; Fig. 4 and Fig. 5, c and e). Although the short recruitment interaction durations could not be logically excluded, these were unexpected. This finding necessitates the reevaluation of our basic concept on how signaling exactly occurs in living cells (see Fig. 8 in Suzuki et al., 2007).

The recruitment of single Lyn molecules to CD59 clusters takes place without any temporal correlation with the occurrence of STALL (Figs. 4 and 5), although Lyn activation is required for STALL. In contrast, a CD59's STALL and its Gai2 recruitment are temporarily highly correlated: STALL is initiated right after the recruitment of each Gai2 molecule. Furthermore, pharmacological blocking of Gai2 inhibited STALL. Collectively, these results suggest that when Gai2 is recruited to a CD59 cluster (and because Lyn is recruited often), it may bind to and activate the recruited Lyn (Ma et al., 2000) at the CD59 cluster, during the short residency periods of both molecules (the colocalization of Lyn and Gai2 at CD59 clusters was shown at the immunofluorescence level in Figs. 6 and 7). The direct, single-molecule detection of Gai2 binding to Lyn and

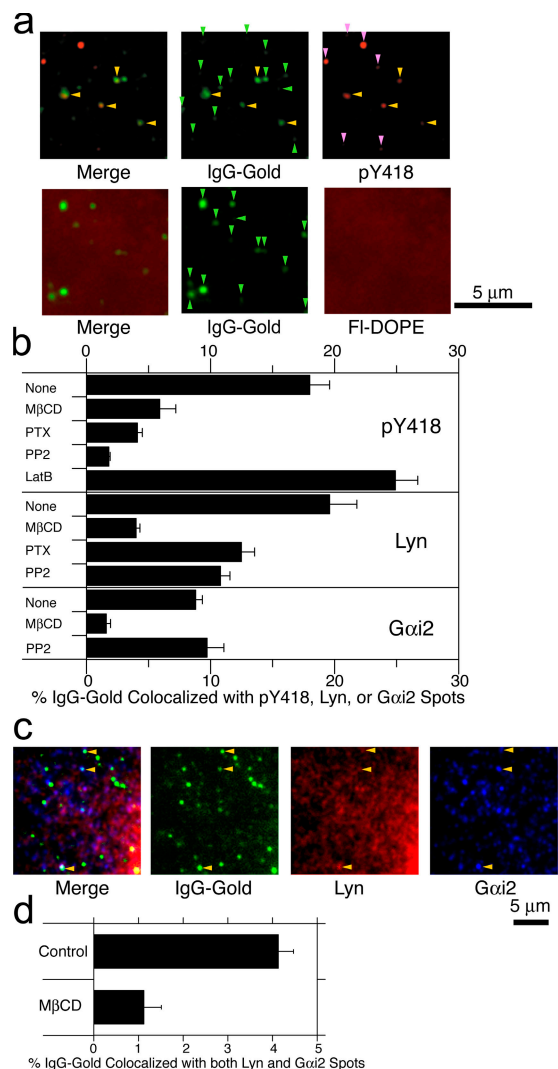


Figure 7. **Immunofluorescence colocalization of IgG-gold particles with immunostained spots formed by anti-pY418 (actually Y397 for Lyn, the phosphorylation of which enhances its activity), anti-Lyn, and anti-Gai2 antibodies.** (a, top) Some of the CD59 clusters formed by IgG-gold particles (green; stained with fluorescein-conjugated secondary antibodies) are colocalized by anti-pY418 spots (red). Lookup tables similar to that in Fig. 1 c were used. Yellow arrowheads indicate colocalized IgG-gold and anti-pY418 spots. Light green and pink arrowheads indicate IgG-gold and anti-pY418 spots, respectively, that do not show colocalization with each other. (bottom) Fluorescein-DOPE is not concentrated at the IgG-gold particles. (b) The fraction of IgG-gold particles colocalized by the anti-pY418, -Lyn, or -Gai2 spots before and after various pretreatments. (c) Some of IgG-gold particles (green) are colocalized by both anti-Lyn and -Gai2 spots (red and blue, respectively). Yellow arrowheads indicate colocalized IgG-gold, Lyn, and Gai2 spots. (d) The fraction of IgG-gold particles colocalized by both anti-Lyn and anti-Gai2 spots before and after the pretreatment with MβCD. Error bars indicate SEM.

the subsequent Lyn activation at a CD59 cluster is one of the key remaining issues for future studies.

The recruitment of Gai2 and Lyn to CD59 clusters might be mediated by a transmembrane protein (Fig. 8, X), and the recruitment of protein X might be facilitated by raft-based interactions (Suzuki et al., 2007). The recruitment of Lyn and Gai2 to CD59 clusters might also be mediated by raft domains located in the two leaflets, perhaps because of interdigitation

(Simons and Ikonen, 1997; Kusumi et al., 2004; Kiessling et al., 2006). The latter interaction may be weak but sufficient to cause or facilitate brief recruitments for 0.1–0.2 s. The involvement of raft-based lipid–lipid interactions in these processes, as suggested by the recruitment of LynN20-GFP to CD59 clusters (although at lower frequencies; Table IV), in addition to protein–protein interactions, will be comprehensively discussed by Suzuki et al. (2007).

How Lyn activation leads to STALL of CD59 clusters remains unknown

Partial depolymerization of actin filaments blocked the STALL of CD59 clusters (Table I), which suggests the binding of CD59 clusters to actin filaments (indirectly, by way of a third protein) or to membrane domains supported by actin filaments. Interestingly, Lyn activation was not blocked by partial actin depolymerization (Table I and Fig. 2 c), suggesting that Lyn activation may occur upstream of the interactions of CD59 clusters with actin filaments. The activated Lyn might phosphorylate an as-yet-unknown protein, X or Y (transmembrane or cytoplasmic surface-associated; Fig. 8), which may trigger the binding of CD59 clusters to an actin filament and/or an actin-dependent membrane domain, inducing STALL. In Suzuki et al. (2007), we show that STALL sites are the key, but transient, sites where PLC γ 2 molecules are recruited to produce IP $_3$, leading to intracellular Ca $^{2+}$ mobilization. Lyn (or Lyn–Gai2 complex) leaves the CD59 cluster very quickly (Figs. 4 and 5), and it may continue to be active outside the CD59 cluster. Therefore, in future studies, it would be interesting to examine how activated Lyn behaves after it leaves the CD59 cluster.

Materials and methods

Cell culture, drug treatments, and cDNA transfection

T24 (human) and PitK2 (rat kangaroo) epithelial cells and NRK (rat) fibroblastic cells were cultured in HAM's F12 medium (Invitrogen) supplemented with 10% FBS. The T24 cell line is, unlike most immune cells, easily amenable to single fluorescent molecule tracking experiments using a total internal reflection fluorescence (TIRF) set up, because it attaches to the coverslip and has flat parts in the upper plasma membrane and transfection and cloning of T24 cells are generally straightforward.

SYF mouse embryonic fibroblast cells (Klinghoffer et al., 1999), which lack c-Src, Fyn, Yes, and Lyn, and YF cells, which express c-Src, but not Fyn, Yes, or Lyn, were cultured in DME (Invitrogen) containing 10% FBS. The PitK2, NRK, SYF, and YF cells were transfected with the cDNA for human CD59. These cells express CD59 of their own species, but to carry out experiments under similar clustering conditions, they were transfected with the human cDNA for CD59. To examine the involvement of Lyn in STALL induction, SYF cells were transfected with the cDNA for Lyn fused with GFP at the C terminus (Lyn-GFP); this GFP construct is known to be functional (Kovarova et al., 2001). Transfection was performed using Lipofectamine Plus (Life Technologies) according to the manufacturer's recommendations.

Partial depletion of cholesterol in the plasma membrane was performed by incubating the cells in 4 mM M β CD (Sigma-Aldrich) at 37°C for 30 min (Kilsdonk et al., 1995) or in 60 μ g/ml saponin (Sigma-Aldrich) on ice for 15 min (Cerneus et al., 1993). These treatments substantially increased the amount of CD59 recovered in the detergent-soluble fractions in the protocol to prepare DRM. Replenishment of cholesterol was performed by incubating the cholesterol-depleted cells in 10 mM M β CD–cholesterol complex (1:1) for 30 min at 37°C (Shigematsu et al., 2003). The overall amounts of cholesterol per cell after cholesterol depletion with M β CD and after the subsequent replenishment were found to be 66 and 118% of the original amount (SD of \pm 6%), as determined by a cholesterol E-test kit (Wako). Partial actin depolymerization was performed by incubating the cells in

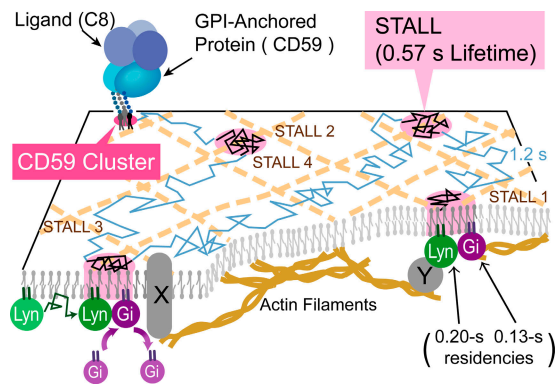


Figure 8. A model showing how the recruitment of Lyn and Gai2 at a CD59 cluster might induce its STALL. The recruitment of Gai2 and Lyn to the same CD59 cluster induces the binding of Gai2 and Lyn, activating Lyn. This might lead to phosphorylation of as-yet-unknown proteins, X or Y (transmembrane or cytoplasmic surface associated), triggering the binding of the CD59 cluster to an actin filament and/or an actin-dependent membrane domain, inducing STALL.

medium containing 50 nM latrunculin B for 10 min [gifts from Dr. G. Marriott, University of Wisconsin–Madison, Madison, WI; Spector et al., 1983]. SFKs were inhibited by treating the cells with 10 μ M PP2 (Calbiochem) for 5 min at 37°C (Hanke et al., 1996). Heterotrimeric G protein was inhibited by incubating the cells in medium containing 1.7 nM PTX (Calbiochem) at 37°C for 22 h (Gomez-Mouton et al., 2004).

To visualize caveolae and coated pits, T24 cells were transfected with caveolin 1–GFP cDNA (a gift from T. Fujimoto, Nagoya University Medical School, Nagoya, Japan; Pelkmans et al., 2001) and AP2 α -GFP (a gift from J. Keen, Thomas Jefferson University, Philadelphia, PA), respectively. Their distributions in the cell totally overlapped with the fluorescent spots after immunostaining with anti-caveolin 1 and anti-clathrin antibodies, respectively, suggesting that their distributions faithfully represent those of caveolae and clathrin-coated pits. The bright-field image of gold particles and cells and the fluorescence image of GFP were simultaneously observed.

As a control for GPI anchoring, a transmembrane chimeric protein of CD59 was used (mycCD59TM; its cDNA was provided by M. Maio, Istituto Nazionale di Ricovero e Cura a Carattere Scientifico, Ancona, Italy): the CD59 ectodomain was fused with an N-terminal myc tag and a C-terminal LDL receptor transmembrane domain, which additionally contains the 12 amino acids from the N terminus of the cytoplasmic domain of the LDL receptor (and thus lacks the sequence required for internalization via coated pits; De Nardo et al., 2002). IgG-gold particles coated with anti-myc antibody (9E10.2) were used for cross-linking mycCD59TM.

To examine the role played by the lipid anchoring chains of Lyn in its recruitment to CD59 clusters, the cDNA for LynN20-GFP, the N-terminal 20-amino-acid sequence of Lyn, which contains the binding sites for palmitoyl and myristoyl chains, fused at its C terminus to GFP, was prepared (Pyenta et al., 2001), and T24 cells were transfected with the LynN20-GFP cDNA.

Immunofluorescence colocalization experiments

Immunofluorescence staining of IgG-gold particles (stained with fluorescein-conjugated secondary antibodies to the mouse anti-CD59 antibody), and their colocalization with immunofluorescent spots of anti-pY418, -Gai2, and -Lyn, was examined in the following way. Cells were incubated with IgG-gold for 5 min at 37°C, fixed with 4% paraformaldehyde for 90 min at room temperature, and permeabilized with 0.01% Triton X-100 in PBS for 1 min. After blocking with 5% skim milk for 90 min, the cells were immunostained with the rabbit anti-pY418, -Gai2, or -Lyn antibodies (Santa Cruz Biotechnology, Inc.).

For the three-way colocalization, i.e., IgG-gold particles with Lyn and Gai2 spots, the following method was used. IgG-gold particles were stained with fluorescein-conjugated secondary antibodies to the mouse anti-CD59 antibody (Cappel). Lyn was stained with sheep biotinylated anti-Lyn antibody (Abcam) and rhodamine-avidin (Vector Laboratories), and Gai2 was labeled with rabbit anti-Gai2 antibodies (Santa Cruz Biotechnology, Inc.) and Cy5-conjugated goat anti-rabbit antibodies (Jackson ImmunoResearch Laboratories).

Immunofluorescence colocalization of large CD59 clusters, formed by the successive addition of primary and secondary antibodies, with the immunofluorescent spots of Gai2 and Lyn, were performed as follows. The cells were washed with HBSS twice and were incubated with 10 µg/ml anti-CD59 monoclonal antibody (MEM43/5 mouse monoclonal antibody, a gift from V. Horejsi, Academy of Sciences of the Czech Republic, Prague, Czech Republic) in the same solution for 10 min at 37°C. After the cells were washed with HBSS, a 10 µg/ml solution of fluorescein-conjugated secondary antibodies (produced in goat) to mouse IgG (Cappel) was added and incubated with the cells for 10 min at 37°C. The cells were fixed with 4% paraformaldehyde for 90 min at room temperature, permeabilized with 0.01% Triton X-100 in PBS for 1 min, quenched with 5% skim milk for 60 min, and, after washing, immunostained with rabbit antibodies for Gai2 or Lyn (Santa Cruz Biotechnology, Inc.) and rhodamine-conjugated goat antibodies to rabbit IgG (Cappel). For the three-way immunocolocalization of Gai2, Lyn with IgG-gold (CD59 clusters), the fixed cells were immunolabeled with anti-Gai2 rabbit antibodies and biotinylated sheep antibodies for Lyn (Abcam) and then with Cy5-conjugated goat antibodies to rabbit IgG (Jackson ImmunoResearch Laboratories) and rhodamine-conjugated avidin (Vector Laboratories). Epifluorescence images of IgG-gold, Gai2, and Lyn were obtained with a microscope (IX70; Olympus) equipped with a 60× 1.4 NA objective lens (Plan Apo) and a cooled charge-coupled device (CCD) camera (Quantix; Photometrics). All of the images in a set of experiments were acquired and processed identically for each fluorophore, using MetaVue 6.2 (Universal Imaging Corp.) and Photoshop 5.0 (Adobe). Quantitative results were shown as means ± SEM, with several independent measurements in parentheses.

Preparation of gold and fluorescent probes

Fab-gold particles (40 nm in diameter) were prepared as reported previously (Fujiwara et al., 2002). For the preparation of Fab-gold for labeling CD59 (but not triggering the cellular signaling responses) or DOPE (conjugated to fluorescein, which was used as a tag, rather than a fluorescent probe; Invitrogen), one third of the minimal protecting amount of anti-CD59 Fab (MEM43/5 mouse monoclonal antibody; a gift from V. Horejsi), anti-PLAP Fab (rabbit polyclonal antibodies; Zymed Laboratories), anti-DAF Fab (III6 mouse monoclonal antibody; a gift from V. Horejsi), or anti-fluorescein Fab (rabbit polyclonal antibodies; Invitrogen) was added to the colloidal gold suspension, and the mixture was incubated on a slowly tumbling shaker for 1 h at room temperature. The gold probe was further stabilized with 0.03% Carbowax 20 M (Sigma-Aldrich). After three washes by sedimentation and resuspension in 0.03% Carbowax 20 M/2 mM phosphate buffer, the gold particles were finally resuspended in HBSS containing 0.03% Carbowax 20 M and were used within 6 h. To further suppress the cross-linking by Fab-gold, a final concentration of 8.3 µg/ml of free Fab (which was not bound to gold particles) was premixed with the coated gold particle suspension, and the mixture was added to the cells cultured on coverslips. The ligand for CD59, C8, was added at a cytolitic membrane attack complex unit of 1,000/coverslip (at a serum concentration; Jasin, 1977). For the cross-linking of CD59, PLAP, or DAF, a fivefold minimal protecting amount of anti-CD59 IgG, anti-PLAP IgG, or anti-DAF IgG (whole divalent IgG) was mixed with the gold particle suspension and subjected to the same stabilization and washing procedures as for Fab-gold. For the conjugation of Cy3 with Fab or IgG, a Cy3 monofunctional dye kit (GE Healthcare) was used according to the manufacturer's instructions. The dye/protein ratio was adjusted to ~1 in all cases.

Single-particle tracking of gold probes and single fluorescent molecule tracking of fluorescently labeled proteins

All of the microscopic observations of living cells were performed at 37°C. For single-particle tracking experiments, cells were sparsely seeded on coverslips (4×10^3 cells/coverslip) and were grown for 18–30 h before each experiment. They were used at ~10% confluency. Care was taken to use cells at about the same level of confluency (~10%) for every experiment because the macroscopic diffusion rate in the T24 cell membrane was found to depend on the confluency level (the macroscopic diffusion coefficients for CD59 and DOPE were twofold higher in the confluent cell membranes; note that they were practically the same if the confluency levels were the same). The incorporation of Cy3-DOPE or fl-DOPE into cell membranes was done as previously reported (Fujiwara et al., 2002).

IgG-gold particles were added to the cells at a final concentration of 1.8×10^{10} particles/ml. This concentration was selected so that it is sufficiently high to induce robust intracellular signaling responses, like those after the addition of high concentrations of C8, and yet sufficiently low not to bother single-particle tracking by the close encounters of two particles on the cell surface.

Single-particle tracking of gold probes was performed on the apical/dorsal membrane, using a microscope (E800; Nikon) equipped with a 100× 1.4 NA objective lens and a CCD camera (XC-75; Sony), as described previously (Fujiwara et al., 2002; Suzuki et al., 2005). Single fluorescent molecule tracking was performed using a home-built, objective lens-type, TIRF microscope, based on the same microscope (Murakoshi et al., 2004; Koyama-Honda et al., 2005). The accuracies of the position determinations for stationary probes were estimated from the SDs of the determined coordinates of the probes fixed on poly-L-lysine-coated coverslips impregnated in 10% polyacrylamide gel. The accuracies for the gold and Cy3 probes at 33-ms resolution were ± 2 and ± 17 nm (SD), respectively.

Detection of STALL

The term STALL was used instead of TCZ to avoid confusion, because we were unable to rule out the possibility that the temporary immobilization of CD59 clusters is induced by their binding to the actin-based membrane skeleton, rather than by being confined within preexisting zones. However, the detection of STALL was performed by using the software to detect TCZs, developed by Simson et al. (1995). STALL (TCZ) was detected in gold-probe trajectories recorded at a 33-ms resolution for a period of 10 s, as previously described (Simson et al., 1995). The length of the trajectories used for the analysis had no influence on the estimated parameters, as long as it was > 5 s. The size of the area covered by a CD59 cluster during STALL was estimated by 2D Gaussian fitting of the determined coordinates of the CD59 cluster during the STALL period.

Observation of the recruitment of single molecules of GFP-PLC γ 2, Lyn-GFP, and Gai2(YFP) to the CD59 cluster

To observe the recruitment of Lyn or Gai2 to CD59 clusters in live cells, T24 cells were transiently transfected with the cDNA for Lyn fused with GFP (at the C terminus of Lyn) or with that for Gai2 fused with YFP (which was placed between the 91st and 92nd amino acids of Gai2's; the cDNA for Gai2, obtained from T. Haga, Gakushuin University, Tokyo, Japan, was modified according to Bunemann et al., [2003]). Lyn-GFP has been known to be functional (Kovarova et al., 2001). Yu and Rasenick (2002) and Frank et al. (2005) showed that Gai2(YFP) underwent proper membrane targeting and G $\beta\gamma$ association. Detection of single Lyn-GFP or Gai2(YFP) molecules was confirmed by single-step photobleaching of each individual fluorescent spot, as well as by the single Gaussian distribution of the signal intensity of the fluorescent spots (Koyama-Honda et al., 2005).

For the simultaneous tracking of single CD59 clusters and single molecules of Lyn-GFP or Gai2(YFP), CD59 clusters were formed by using 50-nm latex beads coated with anti-CD59 whole IgG, because the 40-nm gold particles gave signals that could not be separated from the fluorescence signals from GFP or YFP, at the level of single molecules and single particles. These two types of particles exhibited practically the same STALL time fractions and durations. Furthermore, as shown in Fig. 2 b (left) in Suzuki et al. (2007) and the fourth trace from the bottom in Fig. 3 b (Suzuki et al., 2007), these 50-nm beads were capable of inducing intracellular signals as effectively as 40-nm gold IgG-gold particles.

The bright-field images of the 50-nm latex beads (forming CD59 clusters beneath them) were obtained simultaneously with the images of GFP-tagged single signaling molecules, under or near total internal reflection illumination conditions, using an E800 microscope equipped with a high NA objective lens (Apo TIRF 100×; NA = 1.49; Nikon) and two high-sensitivity cameras operating synchronously. The microscope has two detection arms, and they simultaneously receive the signals separated by a dichroic mirror and optical filters placed just before and within the detection arms. One is for single fluorescent molecule imaging and is equipped with an image intensifier lens (C8600-03; Hamamatsu) coupled with an electron bombardment CCD camera (C7190-23; Hamamatsu), or with an image intensifier lens (VS4-1845; VideoScope) coupled to a camera (VE1000 SIT; Dage-MTI). The other arm is for single-bead tracking (bright-field imaging) and is equipped with a CCD camera (XC-75).

Colocalization was determined as described by Koyama-Honda et al. (2005), i.e., when the distance between the center of the bead image and that of the GFP-tagged signaling molecule was < 100 nm, they were regarded as being colocalized. This is a condition where ~98% of bound molecules are classified as colocalized molecules when the binding did occur, under the present signal-to-noise ratio of each image and the present accuracy of superimposing images obtained on two cameras placed on two separate detection arms. The frequency of incidental colocalization events was evaluated by artificially shifting the video sequence for CD59 clusters by 50 frames (1.67 s, which could be an arbitrary period if it is

much longer than the median colocalization period) and was subtracted. The distributions of the time difference (lag time) between the colocalization and the onset of STALL (Fig. 5 a) and the distribution of the colocalization period were obtained. The estimation of colocalization period was not affected by the photobleaching of GFP or YFP because the recruitment durations were substantially shorter than the GFP lifetime before photobleaching and blinking (~850 ms, which was measured for GFP conjugated to stem cell factor receptor, which stays in the plasma membrane). Furthermore, when the laser intensity was increased by a factor of two, the residency times of Lyn-GFP or G α i2(YFP) at CD59 clusters were not significantly affected.

The upper plasma membrane (the membrane facing the buffer rather than the coverslip) was observed throughout this study. This was performed with the TIRF illumination apparatus, but using TIRF at the interface between the medium and the cytoplasm at the upper cell membrane as well as low-angle oblique illumination (see the legend to Video 2). The ability to track single fluorescent molecules on the upper plasma membrane was further confirmed by using 4.5- μ m-diameter anti-CD59 IgG-coated beads. These beads bound to the upper surface, being excluded from the space between the bottom membrane and the coverslip because of their large size, and induced frequent transient recruitment of Lyn-GFP and G α i2(YFP).

Quantitation of the phosphorylation levels of Lyn and other SFKs in their activation loops

Cells, cultured in a 6-cm dish, were incubated with Fab-gold (for nonstimulated CD59) or IgG-gold (for cross-linking CD59) at 37°C for 1, 2, 5, 10, 30, and 50 min; washed twice with PBS; and lysed with 1% NP-40 + 0.1% SDS lysis buffer containing phosphatase inhibitors and protease inhibitors at room temperature. Lyn was immunoprecipitated from the lysate with anti-Lyn antibodies (Santa Cruz Biotechnology, Inc.) and was blotted with anti-pY418-Src antibodies (Biosource International) and anti-Lyn antibodies. For quantitation of the phosphorylation levels of Lyn and other SFKs, the blot was imaged by a CCD camera and the intensity was quantitated by the NIH ImageJ software.

Online supplemental material

Fig. S1 shows the difference between the membrane compartments (corrals) and STALL and oligomerization-induced trapping of membrane molecules within membrane compartments. Fig. S2 shows the diffusion coefficients for the spots containing five anti-CD59 IgG molecules, showing that they are practically immobile. Fig. S3 gives the definition and the detection protocol for STALL. Fig. S4 demonstrates detection of membrane compartments and STALL in the trajectories observed by high-speed single-particle tracking. Fig. S5 shows that STALL sites are not caveolae. Video 1 provides representative movement of a CD59 cluster (IgG-gold particle) recorded at video rate (replayed in real time), showing alternating periods of apparently simple Brownian diffusion and STALL. The original data for the trajectory shown on the right in Fig. 3 a. Video 2 shows single-molecule detection of transient Lyn-GFP recruitment to a CD59 cluster, occurring without temporal correlation with the STALL of the CD59 cluster. Video 3 shows single-molecule detection of transient G α i2(YFP) recruitment to a CD59 cluster, which occurs right before the onset of the STALL of the CD59 cluster. Video 4 shows single-molecule tracking of G α i2(YFP), showing that G α i2(YFP) is recruited from the cytoplasm to the plasma membrane only transiently, i.e., its residency time on the plasma membrane is generally on the order of 0.1 s or less. Online supplemental material is available at <http://www.jcb.org/cgi/content/full/jcb.200609174/DC1>.

We thank V. Horejsi, M. Tone, M. Maio, T. Fujimoto, J. Keen, and T. Haga for the hybridoma for the production of the anti-CD59 monoclonal antibody and the cDNAs for human CD59, CD59TM, caveolin 1-GFP, AP2 α -GFP, and G α i2, respectively. We also thank K. Jacobson for providing the software for TCZ detection and for helpful discussions, Richard G. Anderson for helpful discussions and, particularly, for suggesting experiments using SYF and YF cells, H. Hirano and M. Aihara for antibody purification and Fab production, and J. Kondo for preparing figures.

This research was supported in part by National Institutes of Health grants DK44375 and AI14584 (M. Edidin) and grants-in-aid for scientific research and those on priority areas from the Ministry of Education, Culture, Sports, Science and Technology of Japan (A. Kusumi).

Submitted: 28 September 2006

Accepted: 20 April 2007

References

- Brown, D.A., and J.K. Rose. 1992. Sorting of GPI-anchored proteins to glycolipid-enriched membrane subdomains during transport to the apical cell surface. *Cell*. 68:533–544.
- Brugger, B., C. Graham, I. Leibrecht, E. Mombelli, A. Jen, F. Wieland, and R. Morris. 2004. The membrane domains occupied by glycosylphosphatidylinositol-anchored prion protein and Thy-1 differ in lipid composition. *J. Biol. Chem.* 279:7530–7536.
- Bunemann, M., M. Frank, and M.J. Lohse. 2003. Gi protein activation in intact cells involves subunit rearrangement rather than dissociation. *Proc. Natl. Acad. Sci. USA*. 100:16077–16082.
- Cerneus, D.P., E. Ueffing, G. Posthuma, G.J. Strous, and A. van der Ende. 1993. Detergent insolubility of alkaline phosphatase during biosynthetic transport and endocytosis. Role of cholesterol. *J. Biol. Chem.* 268:3150–3155.
- Chen, Y., W.R. Thelin, B. Yang, S.L. Milgram, and K. Jacobson. 2006. Transient anchorage of cross-linked glycosyl-phosphatidylinositol-anchored proteins depends on cholesterol, Src family kinases, caveolin, and phosphoinositides. *J. Cell Biol.* 175:169–178.
- De Nardo, C., E. Fonsatti, L. Sigalotti, L. Calabro, F. Colizzi, E. Cortini, S. Coral, M. Altomonte, and M. Maio. 2002. Recombinant transmembrane CD59 (CD59TM) confers complement resistance to GPI-anchored protein defective melanoma cells. *J. Cell. Physiol.* 190:200–206.
- Dietrich, C., B. Yang, T. Fujiwara, A. Kusumi, and K. Jacobson. 2002. Relationship of lipid rafts to transient confinement zones detected by single particle tracking. *Biophys. J.* 82:274–284.
- Douglass, D., and R.D. Vale. 2005. Single-molecule microscopy reveals plasma microdomains created by protein-protein networks that exclude or trap signaling molecules in T cells. *Cell*. 121:937–950.
- Frank, M., L. Thumer, N.J. Lohse, and M. Bunemann. 2005. G protein activation without subunit dissociation depends on a G α i-specific region. *J. Biol. Chem.* 280:24584–24590.
- Fujiwara, T., K. Ritchie, H. Murakoshi, K. Jacobson, and A. Kusumi. 2002. Phospholipids undergo hop diffusion in compartmentalized cell membrane. *J. Cell Biol.* 157:1071–1081.
- Glebov, O.O., and B.J. Nichols. 2004. Lipid raft proteins have a random distribution during localized activation of the T-cell receptor. *Nat. Cell Biol.* 6:238–243.
- Gomez-Mouton, C., R.A. Lacalle, E. Mira, S. Jimenez-Baranda, D.F. Barber, A.C. Carrera, and A.C. Martinez. 2004. Dynamic redistribution of raft domains as an organizing platform for signaling during cell chemotaxis. *J. Cell Biol.* 164:759–768.
- Gri, G., B. Molon, S. Manes, T. Pozzan, and A. Viola. 2004. The inner side of T cell lipid rafts. *Immunol. Lett.* 94:247–252.
- Hanke, J.H., R.L. Dow, P.S. Changelian, W.H. Brissette, E.J. Weringer, B.A. Pollok, and P.A. Connelly. 1996. Discovery of a novel, potent, and Src family-selective tyrosine kinase inhibitor. *J. Biol. Chem.* 271:695–701.
- Harder, T., P. Scheffele, P. Verkade, and K. Simons. 1998. Lipid domain structure of the plasma membrane revealed by patching of membrane components. *J. Cell Biol.* 141:929–942.
- Iino, R., I. Koyama, and A. Kusumi. 2001. Single molecule imaging of green fluorescent proteins in living cells: E-cadherin forms oligomers on the free cell surface. *Biophys. J.* 80:2667–2677.
- Jasin, H.E. 1977. Absence of the eighth component of complement in association with systemic lupus erythematosus-like disease. *J. Clin. Invest.* 60:709–715.
- Kiessling, V., J.M. Crane, and L.K. Tamm. 2006. Transbilayer effects of raft-like lipid domains in asymmetric planar bilayers measured by single molecule tracking. *Biophys. J.* 91:3313–3326.
- Kimberley, F.C., B. Sivasankar, and B.P. Morgan. 2007. Alternative roles for CD59. *Mol. Immunol.* 44:73–81.
- Kilsdonk, E.P., P.G. Yancey, G.W. Stoudt, F.W. Bangerter, W.J. Johnson, M.C. Phillips, and G.H. Rothblat. 1995. Cellular cholesterol efflux mediated by cyclodextrins. *J. Biol. Chem.* 270:17250–17256.
- Klinghoffer, R.A., C. Sachsenmaier, J.A. Cooper, and P. Soriano. 1999. Src family kinases are required for integrin but not PDGFR signal transduction. *EMBO J.* 18:2459–2471.
- Kmieciak, T.E., and D. Shalloway. 1987. Activation and suppression of pp60c-src transforming ability by mutation of its primary sites of tyrosine phosphorylation. *Cell*. 49:65–73.
- Kovarova, M., P. Tolar, R. Arudchandran, L. Draberova, J. Rivera, and P. Draber. 2001. Structure-function analysis of Lyn kinase association with lipid rafts and initiation of early signaling events after Fc ϵ receptor I aggregation. *Mol. Cell Biol.* 21:8318–8328.
- Koyama-Honda, I., K. Ritchie, T. Fujiwara, R. Iino, H. Murakoshi, R.S. Kasai, and A. Kusumi. 2005. Fluorescence imaging for monitoring the colocalization of two single molecules in living cells. *Biophys. J.* 88:2126–2136.

- Kusumi, A., I. Koyama-Honda, and K. Suzuki. 2004. Molecular dynamics and interactions for creation of stimulation-induced stabilized rafts from small unstable steady-state rafts. *Traffic*. 5:213–230.
- Kusumi, A., Y. Sako, and M. Yamamoto. 1993. Confined lateral diffusion of membrane receptors as studied by single particle tracking (nanovid microscopy). Effects of calcium-induced differentiation in cultured epithelial cells. *Biophys. J.* 65:2021–2040.
- Ma, Y.C., J. Huang, S. Ali, W. Lowry, and X.Y. Huang. 2000. Src tyrosine kinase is a novel direct effector of G proteins. *Cell*. 102:635–646.
- Mashanov, G.I., D. Tacon, M. Peckham, and J.E. Molloy. 2004. The spatial and temporal dynamics of pleckstrin homology domain binding at the plasma membrane measured by imaging single molecule in live mouse myoblasts. *J. Biol. Chem.* 279:15274–15280.
- Minshall, R.D., C. Tiruppathi, S.M. Vogel, W.D. Niles, A. Gilchrist, H.E. Hamm, and A.B. Malik. 2000. Endothelial cell-surface gp60 activates vesicle formation and trafficking via G(i)-coupled Src kinase signaling pathway. *J. Cell Biol.* 150:1057–1070.
- Miotti, S., M. Bagnoli, A. Tomassetti, M.I. Colnaghi, and S. Canebari. 2000. Interaction of folate receptor with signaling molecules lyn and G(alpha)(i-3) in detergent-resistant complexes from the ovary carcinoma cell line IGROV1. *J. Cell Sci.* 113:349–357.
- Morgan, B.P., C.W. van den Berg, E.V. Davies, M.B. Hallett, and V. Horejsi. 1993. Cross-linking of CD59 and of other glycosylphosphatidylinositol-anchored molecules on neutrophils triggers cell activation via tyrosine kinase. *Eur. J. Immunol.* 23:2841–2850.
- Murakoshi, H., R. Iino, T. Kobayashi, T. Fujiwara, C. Ohshima, A. Yoshimura, and A. Kusumi. 2004. Single-molecule imaging analysis of Ras activation in living cells. *Proc. Natl. Acad. Sci. USA*. 101:7317–7322.
- Murase, K., T. Fujiwara, Y. Umemura, K. Suzuki, R. Iino, H. Yamashita, M. Saito, H. Murakoshi, K. Ritchie, and A. Kusumi. 2004. Ultrafine membrane compartments for molecular diffusion as revealed by single molecule techniques. *Biophys. J.* 86:4075–4093.
- Murray, E.W., and S.M. Robbins. 1998. Antibody cross-linking of the glycosylphosphatidylinositol-linked protein CD59 on hematopoietic cells induces signaling pathways resembling activation by complement. *J. Biol. Chem.* 273:25279–25284.
- Pelkmans, L., J. Kartenbeck, and A. Helenius. 2001. Caveolar endocytosis of simian virus 40 reveals a new two-step vesicular-transport pathway to the ER. *Nat. Cell Biol.* 3:473–483.
- Pyenta, P.S., D. Holowka, and B. Baird. 2001. Cross-correlation analysis of inner-leaflet-anchored green fluorescent protein co-redistributed with IgE receptors and outer leaflet lipid raft components. *Biophys. J.* 80:2120–2132.
- Sharma, P., R. Varma, R.C. Sarasij, I.G. Krishnamoorthy, M. Rao, and S. Mayor. 2004. Nanoscale organization of multiple GPI-anchored proteins in living cell membranes. *Cell*. 116:577–586.
- Sheets, E.D., G.M. Lee, R. Simson, and K. Jacobson. 1997. Transient confinement of a glycosylphosphatidylinositol-anchored protein in the plasma membrane. *Biochemistry*. 36:12449–12458.
- Shenoy-Scaria, A.M., J. Kwong, T. Fujita, M.W. Olszowy, A.S. Shaw, and D.M. Lubin. 1992. Signal transduction through decay-accelerating factor. Interaction of glycosyl-phosphatidylinositol anchor and protein tyrosine kinases p56lck and p59fyn. *J. Immunol.* 149:3535–3541.
- Shigematsu, S., R.T. Watson, A.H. Khan, and J.E. Pessin. 2003. The adipocyte plasma membrane caveolin function/structural organization is necessary for the efficient endocytosis of GLUT4. *J. Biol. Chem.* 278:10683–10690.
- Simons, K., and G. van Meer. 1988. Lipid sorting in epithelial cells. *Biochemistry*. 27:6197–6202.
- Simons, K., and E. Ikonen. 1997. Functional rafts in cell membranes. *Nature*. 387:569–572.
- Simons, K., and D. Toomre. 2000. Lipid rafts and signal transduction. *Nat. Rev. Mol. Cell Biol.* 1:31–39.
- Simson, R., E.D. Sheets, and K. Jacobson. 1995. Detection of temporary lateral confinement of membrane proteins using single-particle tracking analysis. *Biophys. J.* 69:989–993.
- Solomon, K.R., C.E. Rudd, and R.W. Finberg. 1996. The association between glycosylphosphatidylinositol-anchored proteins and heterotrimeric G protein alpha subunits in lymphocytes. *Proc. Natl. Acad. Sci. USA*. 93:6053–6058.
- Spector, I., N.R. Shochet, Y. Kashman, and A. Groweiss. 1983. Latrunculin: novel marine toxins that disrupt microfilament organization in cultured cells. *Science*. 219:493–495.
- Stefanova, I., V. Horejsi, I.J. Ansotegui, W. Knapp, and H. Stockinger. 1991. GPI-anchored cell-surface molecules complexed to protein tyrosine kinases. *Science*. 254:1016–1019.
- Suzuki, K., K. Ritchie, E. Kajikawa, T. Fujiwara, and A. Kusumi. 2005. Rapid hop diffusion of a G-protein-coupled receptor in the plasma membrane as revealed by single-molecule techniques. *Biophys. J.* 88:3659–3680.
- Suzuki, K.G.N., T.K. Fujiwara, M. Edidin, and A. Kusumi. 2007. Dynamic recruitment of phospholipase Cγ at transiently immobilized GPI-anchored receptor clusters induces IP₃-Ca²⁺ signaling: single-molecule tracking study 2. *J. Cell Biol.* 177:731–742.
- Yu, J.-Z., and M.M. Rasenick. 2002. Real-time visualization of a fluorescent Gαs: dissociation of the activated G protein from plasma membrane. *Mol. Pharmacol.* 61:352–359.